Lawrence Berkeley National Laboratory

Title

Evaluation of a nanoporous lyotropic liquid crystal polymer membrane for the treatment of hydraulic fracturing produced water via cross-flow filtration

Permalink

https://escholarship.org/uc/item/618961br

Authors

Dischinger, Sarah M
Rosenblum, James
Noble, Richard D
et al.

Evaluation of a Nanoporous Lyotropic Liquid Crystal Polymer Membrane for the Treatment of Hydraulic Fracturing Produced Water via Cross-Flow Filtration

Sarah M. Dischinger[a], James Rosenblum[b], Richard D. Noble[a]*, Douglas L. Gin[c]*

[a]Department of Chemical and Biological Engineering, University of Colorado, Boulder, CO 80309, USA
[b]Department of Civil and Environmental Engineering, Colorado School of Mines, Golden, CO 80401, USA
[c]Department of Chemistry, University of Colorado, Boulder, CO 80309, USA

*Corresponding Author

sarah.dischinger@colorado.edu, jrosenblum@mines.edu, richard.noble@colorado.edu, douglas.gin@colorado.edu

Abstract:

Current commercial nanofiltration and reverse osmosis membranes are limited in scope and performance due to their physicochemical properties. Desalination of hydraulic fracturing wastewater poses a particular challenge to membrane filtration given the high concentrations of both organic compounds and salts present in these waters. The recently-developed nanoporous, bicontinuous cubic, lyotropic liquid crystal, thin-film-composite polymer membrane (TFC Q_I membrane), having unique physicochemical properties, enables an alternative treatment of hydraulic fracturing wastewater. Specifically, the TFC Q_I membrane recovers the organic compounds from this high-salinity wastewater, enabling biodegradation to occur after desalination. However, other performance criteria must be demonstrated for a membrane to reach application. The work presented herein demonstrates the stable performance of the TFC Q_I membrane during 66 h of cross-flow filtration of hydraulic fracturing produced water. Compared to the commercial NF90 membrane, the TFC Q_I membrane recovered a larger portion of the organic compounds, had a higher thickness-normalized water flux, and fouled less. The combination of the TFC Q_I membrane's selectivity with its reduced fouling propensity makes possible a treatment for hydraulic fracturing wastewater and other complex aqueous streams inaccessible by most commercial membranes, motivating the further study and development of the TFC Q_I membrane.

Keywords: nanofiltration; membrane selectivity; hydraulic fracturing; produced water; membrane fouling

Graphical Abstract-
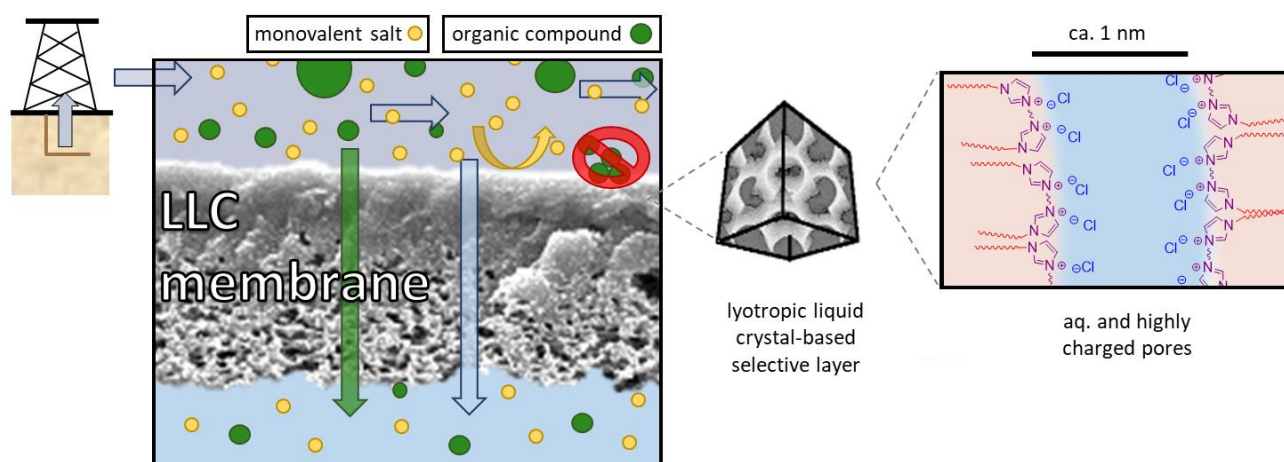
*Reproduced in part from Carter, et al., *Chem. Mater.* **2012**

1. Introduction

Nanofiltration (NF) and reverse osmosis (RO) membrane processes have emerged as efficient approaches for the aqueous fractionation of molecular solutes and water desalination. Membrane processes are advantageous due to their relatively low energy requirements and small, mobile footprint [1–4]. For these reasons, a variety of industries use membrane filtration for food and beverage production, pharmaceutical production, and water purification [5,6]. Despite the increase in use and range of applications for membrane technologies, the variety of chemistries used in membrane materials is still limited – most RO and NF membranes utilize a polyamide-based selective layer [4,6,7]. The physicochemical properties of polyamide-based membranes limit the scope of the industry; two of the most significant limitations arising from these properties are selectivity and propensity for fouling [4,8].

The selectivity of a membrane describes the transport of one molecule relative to another and represents the membrane's ability to separate these components. The limited selectivity of current commercial polymeric membranes results in part from their pore-size distribution, an artifact of the membrane fabrication method [5,9]. Additionally, membranes usually fractionate solutes based on molecular size and thus rarely separate solutes of similar size [8].

Fouling is the build-up of organic or inorganic solids on the membrane surface or within the membrane pores that reduces flux through the membrane [6,9]. Three main factors influence fouling: the composition of the feed water, the hydrodynamic conditions during filtration, and the physicochemical properties of the membrane [10]. Membrane surface roughness and hydrophobicity have been associated with higher fouling propensity [11,12]. Overcoming the

limitations of fouling propensity and selectivity associated with current commercial membranes requires the development of new membrane materials [4].

The recently-developed nanoporous, bicontinuous cubic (Q_I), lyotropic liquid crystal (LLC), thin-film composite (TFC) polymer membrane (TFC Q_I membrane) (Figure 1) is a nanofiltration membrane with unique selectivity and the potential for reduced fouling. The nanostructure of the TFC Q_I membrane consists of highly-charged, ca.-1-nm discrete pores of uniform size [13] defined by periodic hydrophilic and hydrophobic regions. The periodic, phase-separated regions are formed by the self-assembly of an amphiphilic monomer (i.e., having a cationic head group and alkyl, hydrophobic tails) in combination with a polar solvent. Due to the 3D cubic symmetry of the Q_I phase, the hydrophilic regions connect continuously throughout the bulk of the material without requiring alignment, creating a hydrophilic pore system in which water and solutes pass through the material. The cationic head groups form the interface between the hydrophilic and hydrophobic regions (Figure 1), resulting in high charge density within the pore. With this small, highly-charged pore, the TFC Q_I membrane rejects salts, even monatomic salts such as sodium chloride, while allowing the passage of uncharged, low-molecular-weight organic solutes [13]. The ratio of salt rejection to organic solute passage observed in the TFC Q_I membrane is not commonly observed in commercial RO and NF membranes [13,14]. This selectivity, in conjunction with the narrow pore-size-distribution of this LLC polymer material, results in the unique solute rejection performance of the TFC Q_I membrane.
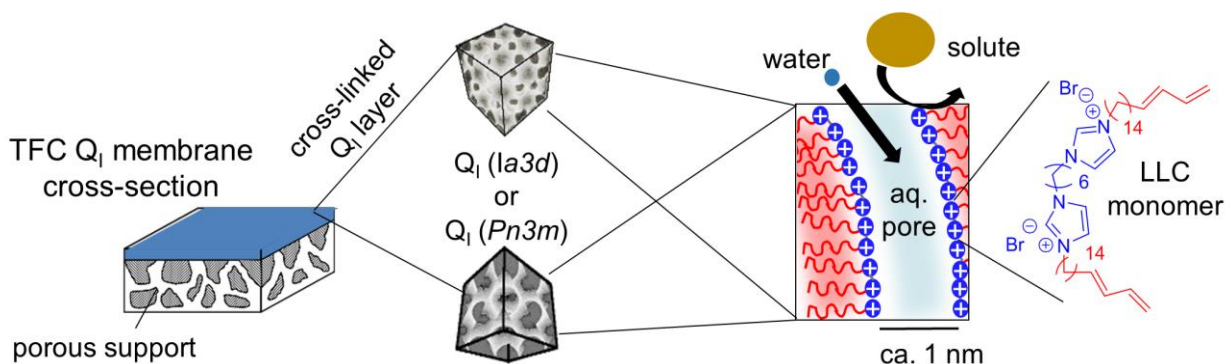
Figure 1. The TFC Q_I membrane, consisting of a cross-linked Q_I LLC selective layer on top of a porous support. The aqueous pore within the Q_I phase has a pore wall formed by the cationic imidazolium head groups present in the LLC monomer. Partially reproduced from References 13 and 14 with permission. Copyright American Chemical Society, 2012; and copyright Elsevier, 2017.

In addition to enabling an alternative selectivity, some of the physicochemical properties of the TFC Q_I membrane suggest that the membrane has a reduced fouling propensity. Quaternary ammonium-based polymers have a similar resistance to protein adsorption as poly(ethylene glycol)-based polymers, which have good anti-fouling properties [15,16]. The imidazolium functional group present in the TFC Q_I membrane is similar to the quaternary ammonium functional group, suggesting the membrane will have a high resistance to fouling as well. Additionally, the presence of a periodic nanostructure significantly decreases protein adsorption compared to an amorphous material of the same chemical composition [15]. The TFC Q_I membrane has a periodic nanostructure similar to that of the previously tested material, suggesting the TFC Q_I membrane also has reduced fouling propensity. In summary, the TFC Q_I membrane, with its unique selectivity and reduced fouling propensity, offers an alternative approach to some of the challenges facing traditional membrane filtration. The treatment of hydraulic fracturing wastewater is one such challenge.

Unconventional oil and gas processes, specifically hydraulic fracturing, may use 4–7 million gallons of water per well. A portion of this 4–7 million gallons returns to the earth's surface with oil and gas as produced water (PW), which is a complex mixture of inorganic constituents, naturally-occurring radioactive material, and organic constituents from both the formation and the injected fluid (i.e., fracturing fluid) [17–19]. PW poses a treatment challenge due to its complex composition – it contains high concentrations of both salts (total dissolved solids, TDS) and organic compounds (dissolved organic carbon, DOC) [20–22]. In 2015, more than 95% of hydraulic fracturing wastewater was deep-well injected [23] due to the lack of economic treatment approaches. However, deep-well injection has been associated with an increase in seismic activity and a reduction in the surface-water quality downstream from these injection sites [23,24], motivating the development of innovative treatment methods and alternative management strategies for this waste stream [25].

Membrane processes offer a desalination method for select PWs. However, the selectivity inherent to commercial polymeric membrane materials compromises their potential contribution to the treatment of this wastewater. NF and RO membranes capable of removing a significant portion of the salinity also remove a significant portion of the DOC at the same time [25–28]. While such a treatment would generally be a desired outcome, many PWs contain high-value products, both inorganic (e.g., iodide and rare earth metals) and organic (e.g., organic acids) [17,29,30]. Directing such products to the concentrate (i.e., waste stream) fails to gain value from them. For example, the DOC in many of these wastewater streams contains a significant concentration of low-molecular-weight and biodegradable organic compounds such as acetate [17,31,32]. Recovered acetate could be used in other refining steps [30]. The biodegradable organics could act as a nutrient source for biological growth and thereby be converted into bio-

based plastics or fuels. Biodegradation of DOC before desalination is challenging because the high salinity present in PW significantly reduces or even prevents biological metabolism [33–35]. Biodegradation of the DOC after desalination would be advantageous because it would enable a wider range of microbial species to consume the DOC and convert the DOC into a valued product. A membrane with the ability to isolate the biodegradable DOC from the high-salinity environment of PW would present an alternative way of thinking about membrane-based treatment, in which desalination comes before biodegradation. However, such a treatment train would require exposing the membrane to high concentrations of organic compounds, an environment problematic for most membranes.

In the presence of high concentrations of organic compounds, membrane performance typically drops quickly due to fouling [25,36,37]. Efforts to mitigate membrane fouling during the treatment of PW include reducing the fouling propensity of the membrane itself [3], utilizing various pretreatment steps [28,38–40], and implementing alternative membrane processes such as forward osmosis [41,42]. However, the pretreatment methods do not enable utilization of the organic fraction, and forward osmosis processes still experience fouling [41]. With a selectivity for low-molecular-weight organic compounds over salts and a promise of a lower fouling propensity, the TFC Q_I membrane offers an opportunity to recover the organic fraction in PW that is not possible with other membranes.

A proof-of-concept study investigated a treatment approach for hydraulic fracturing flowback water utilizing the selectivity afforded by the TFC Q_I membrane [14]. This recent work shows that during the filtration of flowback water, the TFC Q_I membrane recovered the low-molecular-weight organic fraction of the DOC in the permeate while rejecting a large portion of the salinity. The TFC Q_I membrane's performance was compared to a commercial RO

membrane (SW30HR by Dow Filmtec), which rejected both salts and organic compounds to a high degree, and a commercial NF membrane (NF270 by Dow Filmtec), which rejected organic solutes to a similar degree as the TFC Q_I membrane but had a poor rejection of salts. Furthermore, the DOC in the permeate was highly biodegradable. From these results, an alternative treatment approach was proposed in which biological degradation follows desalination. While this proof-of-concept study was conducted on a small scale in dead-end filtration, it provided the motivation for further investigation of the TFC Q_I membrane as a treatment for hydraulic fracturing wastewater.

The TFC Q_I membrane's recent development requires the evaluation of its novel treatment of hydraulic fracturing wastewater in a more-industrially-relevant context. Therefore, the goals of this research were threefold: The first goal was to evaluate the TFC Q_I membrane's selectivity in a more industrially-relevant context, namely cross-flow filtration. The second goal was to evaluate the stability of the TFC Q_I membrane during 66 h of filtration. The third goal was to evaluate the fouling of the TFC Q_I membrane. These goals were accomplished by observing the TFC Q_I membrane's performance during filtration of PW and comparing its performance to that of NF90, a commercial NF membrane produced by Dow Filmtec that has been studied in the literature as a treatment for produced and flowback water [39]. The NF90 membrane was expected to have a DOC rejection more similar to the TFC Q_I membrane than the previously studied SW30HR membrane while having a much higher rejection of TDS than the previously studied NF270 membrane, thereby making the NF90 membrane a more suitable comparison for the TFC Q_I membrane. While other LC-based membranes have been evaluated in cross-flow systems [43,44], the work presented here is the first cross-flow study of this TFC Q_I membrane as well as its first fouling study. Therefore, this work progresses the application of the

TFC Q_I membrane for the treatment of hydraulic fracturing wastewater while motivating the further study of the TFC Q_I membrane's physicochemical properties in relation to its unique performance.

2. Experimental

2.1 PW location and characterization

The PW sample was taken from a horizontal well in the Denver-Julesburg Basin. The well resides in northeastern Colorado, in the Niobrara formation. The sample was taken 3 years after the well was flowed back. The sample was collected from the separator onsite into a 5-gal HDPE carboy and stored at 4 ˚C prior to treatment and analysis. The Laboratory for Environmental and Geological Studies (LEGS) at the University of Colorado Boulder conducted inorganic ion and metal analyses on the PW sample. Metals and trace elements were measured using inductively coupled plasma-mass spectrometry (ICP-MS, Perkin Elmer SCIEX Elan DRC-e), while anions were measured by ion chromatography (Dionex Series 4500I).

2.2 Materials

TFC Q_I membrane samples were fabricated and characterized as previously published [13,14], using the ultrafiltration polysulfone support, PS35 (20 kDa MWCO) purchased from Nanostone Water, Inc. A commercial reference NF membrane, NF90 (Dow Filmtec), was purchased as dry, flat-sheet membrane from Sterlitech and stored sealed until use. The ultrafiltration membrane BY (Synder, 100 kDa MWCO, PVDF) was purchased from Sterlitech as a dry, flat-sheet membrane and stored sealed until use. Microfiltration membranes were

purchased as 0.45 µm high-capacity Dispos-a-Filters from Geotech. Sodium chloride (>99.0%), sodium hydroxide (>97.0%), and hydrochloric acid (36.5–38.0%) were purchased from Fisher Scientific and used as received. Ethanol (90%) was purchased from Deacon Laboratories and used as received. De-ionized (DI) water having a conductivity below 1.5 µS/cm was used.

2.3 Cross-flow filtration system

The cross-flow system (schematic in Figure D1 in the Data in Brief) used for these experiments was a custom-built, bench-scale system. The feed solution was stored in a 4-L HDPE feed tank and gravity fed to a positive displacement pump (Hydracell, M-03S). The pump directed the water through a stainless-steel cross-flow membrane cell (Sterlitech, CF042) and returned the concentrate to the feed tank. The membrane cell had an active area of 42 cm^2 and contained a 23–33 mil PTFE feed spacer (Sterlitech). A backpressure regulator (Tescom, 54-2167T24) controlled the pressure of the feed. Pressure gauges (Swagelok) on either side of the membrane cell measured pressure drop across the membrane cell. In all experiments, however, the pressure drop across the membrane cell was negligible, and the pressure gauge on the inlet side of the membrane cell was used for all pressure readings. A variable frequency drive (Emmerson) controlled the flow rate through the system by regulating the pump speed. A flow meter (Blue-White Industries, Ltd.) in the concentrate line measured the flow rate. A heat exchanger submerged in a refrigerated water bath (VWR International) cooled the concentrate before it returned to the feed tank. A stir rod in the feed tank continuously mixed the returning concentrate with the feed to maintain a uniform feed concentration, and a thermometer measured the temperature of the feed solution.

2.4 Pretreatment of the PW

In order to remove the suspended solids from the raw PW, an I/P series peristaltic pump (Masterflex®) pushed the raw PW through a 0.45-µm Dispos-a-Filter. Ultrafiltration by the BY membrane during cross-flow filtration removed the remainder of the suspended solids. The cross-flow system (see Figure D1 in the Data in Brief) was run at a cross-flow velocity of 20 cm/s, a transmembrane pressure (TMP) of 80 psi, and a temperature of 20 °C. Due to a total volume of 3.5 L, the cross-flow filtration system required multiple batches in order to process the 17 L of microfiltered PW. The ultrafiltration process first concentrated the entire volume at 50% recovery, and then filtered the remaining concentrate further to achieve an overall recovery of 92%. The UF membrane was replaced as needed to maintain a reasonable permeate flux, which decreased over time due to fouling. The permeate was collected in 1-L or 500-mL glass jars (which were muffled at 550 °C for 3 h) and stored at 4 °C. To ensure uniformity of the UF permeate used for all sequential experiments, all the UF permeate (pretreated PW) was combined, mixed, and redistributed to the muffled jars for storage at 4 °C until use.

2.5 Cross-flow nanofiltration of pretreated PW

Before each experiment, 70% aq. ethanol was recirculated through the cross-flow system (Figure D1 in the Data in Brief) for at least 30 min to kill any biological growth present in the system. Then, DI water was recirculated through the system for at least 20 min, replacing the feed solution with fresh DI water at least once. Meanwhile, the membrane to be tested was soaked in DI water for at least 30 min. Once the cross-flow system had been cleaned, the pre-soaked membrane was inserted into the membrane cell. The flow rate was slowly increased until the cross-flow velocity reached a value of (29.0 ± 0.5) cm/s (where the error is 1 standard deviation). The system was then pressurized slowly to a transmembrane pressure (TMP) of (400

± 5) psi (where the error is due to visual reading from the gauge). The refrigeration bath temperature was adjusted to maintain the feed temperature at (20 ± 1) °C (where the error is the maximum deviation measured). The membranes were compacted in DI water at 400 psi for about 23 h.

Previous research shows that the performance of the TFC Q_I membrane varies depending on the anion associated at the pore wall [45,46]. The dominant anion species in PW is chloride (see Table D1 in the Data in Brief). Therefore, anion-exchange of the TFC Q_I membrane to chloride before beginning any experiment was necessary in order to correctly evaluate the impact of PW on the membrane. After compaction, the membrane was exposed to a 0.01 M aq. sodium chloride solution for 9 h. The membrane was then returned to DI water for about 17 h, during which the initial pure water flux was measured. The commercial NF90 reference membrane was treated in an identical manner though exposure to sodium chloride did not significantly change this membrane's performance. Membrane quality was evaluated by pure water flux and by salt rejection during filtration of the 0.01 M aq. sodium chloride solution. Membranes were replaced if they demonstrated a pure water flux outside of the expected range of variation or if they demonstrated a low salt rejection (see Section 2 of the Data in Brief for more information about the quality assessment tests).

After the membrane quality was confirmed, 1.1 L of pretreated PW was recirculated through the cross-flow filtration system under the same conditions as described above (i.e., cross-flow velocity of (29.0 ± 0.5) cm/s, TMP of (400 ± 5) psi, feed temperature of (20 ± 1) °C). The pretreated PW recirculated through the system for about 22 h. The collected permeate was returned to the feed tank in order to maintain a constant feed composition. After 22 h of filtration, the cross-flow membrane cell was isolated and subjected to a clean-in-place (CIP)

process. The CIP process consisted of recirculating 1.2 L of 0.1 M sodium hydroxide through the membrane cell using an I/P series peristaltic pump (Masterflex®) for about 50 min, 1.2 L of 0.1 M hydrochloric acid for 50 min, and DI water for about 15 min. The membrane cell was then reconnected to the cross-flow system, and the system was returned to the desired filtration conditions. The pretreated PW recirculated through the system for another 22 h before being replaced by a fresh 1.1 L of pretreated PW. The fresh pretreated PW recirculated through the cross-flow system for about 22 h. This experimental plan was developed from Riley et al.'s publication using NF90 to treat produced and flowback water [39]. Permeate flux was measured throughout the experiment. Additionally, DOC and TDS concentrations in the feed and permeate were measured via the collection of two 5-mL samples during the final 20 h of filtration. These samples were collected in muffled vials and stored at 4 °C until analysis.

After the 66 h of exposure to pretreated PW, the cross-flow system was returned to DI water. DI water recirculated in the system for about 24 h, and the water flux was measured once the flux stabilized. The membrane was then removed from the cross-flow system and allowed to air-dry for at least 48 h at room temperature. The membrane was stored in a sealed plastic bag until further analysis.

This experimental procedure was used for all NF membrane filtration experiments: NF90 at 400 psi (NF90 (HP)), NF90 at 160 psi (though the membrane was still initially compacted at 400 psi and all other filtration conditions were the same) (NF90 (LP)), and two TFC Q_I membranes at 400 psi (TFC Q_I^A and TFC Q_I^B).

2.6 Adsorption of pretreated PW to nanofiltration membranes

For adsorption tests, the system and membrane were prepared in the same manner as for the nanofiltration experiments, with system pre-treatment, membrane compaction, and membrane quality assessment. At this point, the pure water flux was measured. Then the membrane was exposed to a 15,000 mg/L aq. sodium chloride solution at 0 psi TMP for 1 h. Then the cross-flow system was returned to DI water, pure water flux was measured, and flux recovery after exposure to the high salinity solution was calculated. Then the membrane was exposed to pretreated PW at 0 psi TMP for 1 h. The system was returned to DI water, the pure water flux was measured, and the flux recovery due to exposure to pretreated PW was calculated [47]. The membrane was then removed from the cross-flow cell and allowed to air-dry for at least 48 h. The membrane was then stored sealed in a plastic bag until further characterization. In this set of experiments, the TFC Q_I membrane and one sample of NF90 membrane were exposed to undiluted pretreated PW. Additional samples of NF90 membrane were also exposed to pretreated PW diluted with DI water (1:10 and 1:50; parts pretreated PW: parts total) and then adjusted back to 15,000 mg/L TDS through the addition of sodium chloride. The rational for these adsorption experiments is provided in the results and discussion section.

Given the lack of fresh pretreated PW, the water recovered from the previous filtration experiments was used for adsorption experiments. In all cases, the DOC and TDS concentrations were the same as in the filtration experiments suggesting any differences in water quality due to the previous filtration experiments were negligible. Additionally, the TFC Q_I membrane used for this test did not pass the QA tests, having a salt rejection 5% lower than normal and a PXRD peak (denoting the presence of the periodic LLC structure) slightly outside the expected range. Accounting for these small deviations and the nature of this particular experiment, this membrane was considered sufficient for studying the adsorption properties of the material.

2.7 Calculations

Membrane selectivity was evaluated by observed solute rejection. Observed solute rejection estimates rejection based on the observed feed and permeate concentrations; it does not account for the increased concentration at the membrane surface due to concentration polarization. Observed solute rejection (*Rej*) was calculated using Eq. 1 as shown below:

$$Rej = \left(1 - \frac{C_p}{C_f}\right)$$

Equation 1

where C_p is the concentration of the solute in the permeate, and C_f is the concentration of that solute in the feed. To enable a comparison of each membrane's ability to separate the DOC from the TDS, the salt-organic-separation (SOS) efficiency was calculated as follows [48]:

$$SOS = \frac{Rej_{TDS}}{Rej_{DOC}}$$

Equation 2

Membrane productivity was evaluated by water flux through the membrane. Water flux (*J*) was calculated using Eq. 3 below:

$$J = \frac{V}{At}$$

Equation 3

where *V* is the permeate volume collected during time *t* through membrane area *A*. The uncertainty of the water flux measurements for a given membrane was quantified by one standard deviation of the stabilized pure flux of that membrane. To quantify the change in flux caused by exposure to pretreated PW, the flux was normalized by dividing it by the first flux

measurement collected after the feed was changed to pretreated PW. Flux recovery was

calculated as the ratio of pure water flux after exposure to a given solution and pure water flux

before exposure to that solution.

To enable a better comparison between the intrinsic water transport properties of TFC Q_I

membrane and the NF90 membrane, the flux was normalized to the selective layer thickness (δ)

of each membrane. Equation 4 presents the calculation of the thickness-normalized water flux

(φ):

$$\varphi = J \times \delta$$
<div align="right">Equation 4</div>

Normalizing the flux by the thickness of the selective layer is important because the thickness of

the selective layer varies significantly between the membranes ((0.12 ± 0.01) µm for NF90 [49]

and (3.2 ± 0.6) µm for the TFC Q_I membrane as measured by SEM (see Section 3 of the Data in

Brief)) due to the current fabrication methods. The significant difference in selective layer

between these membranes is apparent in the cross-section images of the two membranes

presented in Figure D3 in the Data in Brief. Given the ongoing development of the fabrication of

the Q_I selective layer, this work focused on the material's intrinsic properties. Therefore, artifacts

of the current fabrication procedure were taken into account to enable a comparison of the

materials themselves.

2.8 Characterization

The periodic nanostructure of all TFC Q_I membrane samples was evaluated using an Inel

CPS 120 PXRD system with a monochromated Cu K_α radiation source. The PXRD system was

calibrated with silicon and silver behenate standards purchased from NIST and Kodak,

respectively [50]. The location of the primary PXRD peak was used as an initial quality assessment of each fabricated Q_I membrane [13,14,45].

The thickness of the selective layer of the TFC Q_I membrane was measured by freeze-fracturing a piece of the TFC Q_I membrane and observing the cross-section using a scanning electron microscope (JEOL JSM-6480LV). Thickness measurements were collected at multiple points from samples collected from 4 different membrane casts.

The theoretical charge density of the TFC Q_I membrane was calculated as shown in Section 3 in the Data in Brief.

2.8.1 Water quality characterization

The concentration of TDS was measured by conductivity using an EC Meter (VWR International) calibrated with a 1000 mg/L standard aq. sodium solution (Hach). A calibration curve ranging from 100 to 1000 mg/L was also made. Samples were diluted into this range using DI water, and the TDS was measured via conductivity. Using conductivity to describe TDS was valid because the majority of the TDS present in this water was sodium chloride (see Table D1 in the Data in Brief) [3]. The concentration of DOC was measured using a Sievers 5310C Laboratory TOC analyzer (GE Analytical Instruments, Inc.). Samples were diluted using DI water into the range of 0.5–15 mg/L in muffled vials. Pre-UF-treated water samples were first passed through a 0.45-µm filter. TSS was measured according to the standard method [51] using a coarse, ground-glass filter (Pall, type A/E). The pH was measured using a Corning pH Meter 320 equipped with a Sensorex combination pH electrode that was calibrated at pH 4, 7, and 10 using standard solutions (Fisher Chemical).

2.8.2 Fouling characterization

Membrane surfaces were imaged with scanning electron microscopy (SEM) using the electron beam of a FEI Nova 600 Nanolab; cross-sections were prepared using a focused ion beam (FIB) of the same FEI Nova 600 Nanolab. All samples were coated in platinum prior to imaging. The qualitative presence of various elements was evaluated using a scanning electron microscope (JEOL JSM-6480LV) with energy-dispersive X-ray spectroscopy (EDS) using Noran EDS software. Sample surfaces were further analyzed using Fourier-transform infrared (FTIR) spectroscopy using a Thermo Scientific Nicolet 6700 spectrometer equipped with a PIKE MIRacle^{TM} single-reflection horizontal attenuated total reflectance (ATR) accessory with a diamond crystal. The water contact angle of dry membranes before and after fouling was measured via the sessile drop method.

3. Results and Discussion

The quality of the raw PW, collected for this study from the Denver-Julesburg Basin in northeastern Colorado, was similar to that of other samples collected from the same basin [14,18,52,53]. The concentrations of ions and trace metals present in the raw PW are provided in Table D1 in the Data in Brief, while the general water quality of the raw PW is provided in Table 1. Compared to water samples collected from basins across the country, this water sample had higher than average DOC concentration and lower than average TDS concentration [3,22,54]. Pretreatment with microfiltration (MF) and ultrafiltration (UF) successfully removed the suspended solids from the raw PW and resulted in a water recovery of 92%. Table 1 also includes the general water quality after each pretreatment step. The resulting pretreated PW, with

high concentrations of TDS and DOC, was used to evaluate the performance of the nanofiltration membranes.

Table 1. Water quality of the raw PW and the water after each pretreatment step. ND means 'not detectable'. Values are averages of at least 2 measurements, with error bars representing 1 standard deviation. Pictures of the raw and pretreated PW samples are presented in Figure D6 of the Data in Brief.

Water	TDS (mg/L)	DOC (mg/L)[a]	TSS (mg/L)	pH
Raw PW	15340 ± 70	256 ± 6	283 ± 7	7.0
MF permeate	15280 ± 9	266 ± 1	7 ± 0	7.3
UF permeate (pretreated PW)	15130 ± 20	291 ± 1	ND	7.7

[a] The observed increases in measured DOC after MF and UF treatment were surprising, and the cause will be examined in follow-up work.

To contextualize performance of the recently developed TFC Q_I membrane, the membrane was compared to the commercial NF90 membrane (Dow Filmtec). Due to the difference in selective layer thickness between these two membranes, the flux through the NF90 membrane was much greater than through the TFC Q_I membrane. Flux was therefore normalized by the selective layer thickness to enable a comparison of the intrinsic water transport properties of the materials. However, the flux also impacts the hydrodynamic environment of filtration and can thereby significantly impact membrane performance and fouling [10,28,36,55]. To account for variation in fouling as a result of the variation in flux, the NF90 membrane was evaluated under two different sets of experimental conditions. In one set of experimental conditions, the NF90 membrane was exposed to the same transmembrane pressure (TMP) as the TFC Q_I membrane (i.e., 400 psi), enabling a comparison of the membranes while exposed to similar driving forces and fouling-layer compaction conditions. This experiment will be referred to as NF90 (HP) to designate it was run at a high TMP. In the second set of experimental conditions,

the NF90 membrane was exposed to a reduced TMP (160 psi) such that the flux through the

NF90 membrane was similar to that of the TFC Q_I membrane; this experiment will be referred to

as NF90 (LP). The filtration experiments discussed below include one NF90 (HP), one NF90

(LP), and duplicate TFC Q_I membrane trials (TFC Q_I [A] and TFC Q_I [B]).

3.1 Selectivity

Solute rejection was used to determine the selectivity of each membrane. The rejection

performances of the TFC Q_I and NF90 membranes are presented in Figure 2. In comparing this

work with previously published work in which the dead-end filtration performance of the TFC Q_I

membrane was explored [14], the TFC Q_I membrane rejected TDS to a similar degree in cross-

flow filtration as in dead-end filtration, but it rejected less DOC in cross-flow filtration than in

dead-end filtration. The difference in DOC rejection is most likely due to the difference in the

organic species present. The similarity in TDS rejection was expected because the major species

of TDS in both waters was sodium chloride. The TDS rejection of the TFC Q_I membrane

demonstrates the membrane's ability to maintain its separation performance in the more-

industrially-relevant context of cross-flow filtration. In comparison to the TFC Q_I membrane in

cross-flow filtration, the NF90 membrane under both high and low TMP rejected more TDS and

DOC. However, the interest herein is in the separation of the DOC from the TDS, and the

rejection results presented in the graph of Figure 2 do not explicitly show which membrane

demonstrated this selectivity.

Selectivity can be quantified by a ratio of solute rejections. Negaresh et al. developed the

salt-organic-separation (SOS) efficiency of NF membranes [48] used by various researchers [56].

The SOS efficiency is calculated using observed rejection and therefore depends on the operating

conditions (e.g., applied pressure, concentration gradient, fouling layer); it does not describe the inherent selectivity of the membrane material. The SOS efficiency calculates the ratio of the observed rejection of the solute retained in the concentrate (herein, TDS) to the observed rejection of the solute passing through the membrane to the permeate (herein, DOC). Therefore, a membrane with a better selectivity for DOC over TDS will have a higher SOS efficiency. Figure 2 includes the SOS efficiency values corresponding to each membrane trial. Comparison of the SOS efficiency values demonstrates that the TFC Q_I membrane had the highest selectivity for DOC over TDS. The permeate quality of the TFC Q_I membrane ((2120 ± 80) mg/L TDS and (180 ± 10) mg/L DOC; the error is 1 standard deviation) was sufficient for the cultivation of microbes for DOC degradation [33] and just above the limit for long-term reuse in agriculture (i.e., 500–2,000 mg/L TDS [17]).
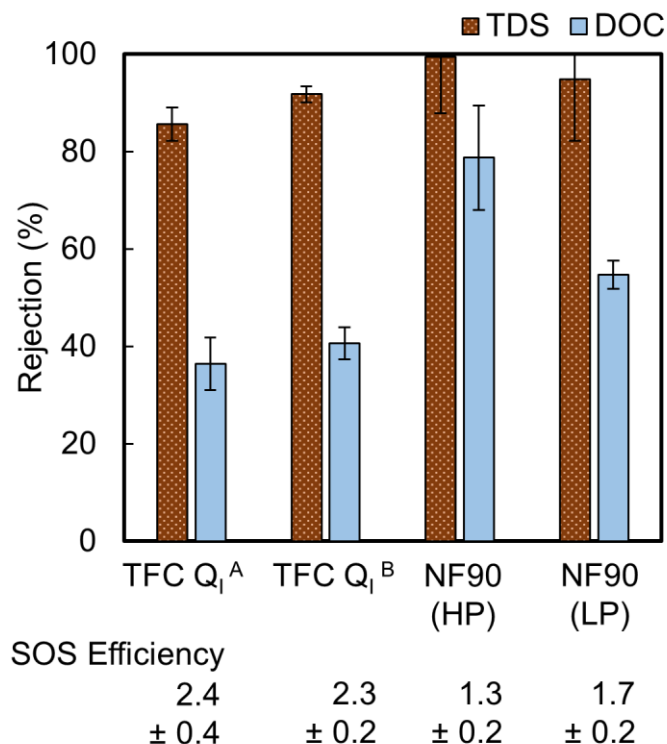
Figure 2. Rejection of TDS and DOC during cross-flow filtration of pretreated PW by the duplicate TFC Q_I membranes at a TMP of 400 psi and by the commercial NF90 membrane at a TMP of 400 psi (NF90 (HP)) and 160 psi (NF90 (LP)). The values are averages of 2 samples
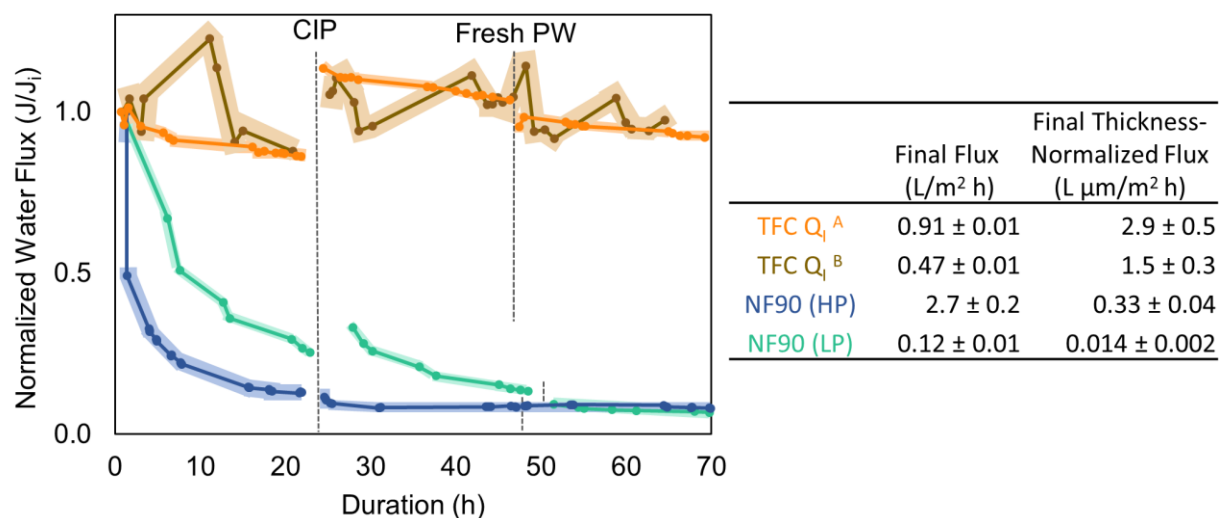
collected in the last 20 h of exposure in each experiment, with error bars representing 1 standard deviation. SOS efficiencies associated with each membrane's performance are included at the bottom and include an error of 1 standard deviation.

3.2 Water flux

Water transport through the TFC Q_I and NF90 membranes was studied in three different ways. First, the water flux was used to describe the water transport of a given membrane, as fabricated and as measured in this system. The water flux was also normalized by thickness of the membrane selective layer to enable a comparison of the intrinsic properties of the material. Finally, the normalized water flux was used to evaluate the change in water flux during the filtration of pretreated PW. The values in the table on the right side of Figure 3 present the final water flux and thickness-normalized water flux measured at the end of each 66-h experiment. While the final water flux of NF90 (HP) was higher than that of either TFC Q_I membrane, it should be noted that the thickness-normalized water flux was actually lower than that of the TFC Q_I membrane. This is important to note because the thickness-normalized flux describes the water transport intrinsic to the material and suggests that, if the TFC Q_I membrane could be fabricated at the same thickness as the NF90 membrane, assuming such a change in fabrication would have no impact on the nanostructure, the TFC Q_I membrane would have a higher flux than the NF90 membrane. This observation suggests that the low flux observed in the TFC Q_I membrane is a fabrication challenge rather than a challenge inherent to the material itself.

The low flux demonstrated by the NF90 membrane during filtration of pretreated PW was not anticipated given the values previously reported [39]. Nonetheless, these NF90 membranes passed the quality assessment tests, demonstrating that they were within specifications prior to the addition of pretreated PW. Direct comparison of the NF90 membrane performance observed herein with its performance found elsewhere in literature is challenging

because of the variation in feed water composition as well as variation in the cross-flow filtration system, both of which can significantly impact the membrane's performance. In this set of experiments, all membranes were exposed to the same feed water in the same cross-flow filtration cell, validating the comparison of the NF90 membrane with the TFC Q_I membrane as presented herein.

	Final Flux (L/m² h)	Final Thickness-Normalized Flux (L µm/m² h)
TFC Q_i A	0.91 ± 0.01	2.9 ± 0.5
TFC Q_i B	0.47 ± 0.01	1.5 ± 0.3
NF90 (HP)	2.7 ± 0.2	0.33 ± 0.04
NF90 (LP)	0.12 ± 0.01	0.014 ± 0.002

Figure 3. Normalized water flux of the TFC Q_I and NF90 membranes when exposed to pretreated PW. 0 h marks initial exposure to pretreated PW. The shaded regions mark one standard deviation of error as evaluated at each data point. The table includes the absolute values of water flux collected at the end of the 66-h exposure, with the error representing one standard deviation.

Figure 3 also includes a graph showing the normalized water flux with duration of filtration of pretreated PW. Flux decline was evident in each membrane trial, demonstrating some degree of fouling occurred in each trial [57]. However, the flux decline through the TFC Q_I membranes was minimal; the TFC Q_I membrane demonstrated a relatively stable performance throughout the duration of the treatment of pretreated PW. The TFC Q_I membrane did experience an increase in water flux after the CIP process. It is unclear from this experiment whether this increase in water flux signifies the removal of the fouling layer or an impact of the

CIP process on the membrane itself, and more explicit testing should be done to elucidate this phenomenon. However, given the relatively constant water flux (Figure 3) and favorable solute selectivity after the CIP process (Figure 2), any degradation to the TFC Q_I membrane due to the CIP process was minimal. Figure 3 shows that the TFC Q_I membrane maintained its performance through the 66 h of exposure to pretreated PW under cross-flow filtration conditions.

Meanwhile, the flux decline in the NF90 membrane at both high and low TMP was dramatic. The greater rate of flux decline in NF90 (HP) than NF90 (LP) is most likely due to the higher initial flux in NF90 (HP) [28,36]. While such a dramatic flux decline by the NF90 membrane was unexpected, it may be explained by heavy fouling due to the high DOC concentration present in this water (NF90 has not, to our knowledge, been exposed to waters with such a high concentration of DOC [37,39,58]).

Flux recovery is a comparison of a membrane's pure water flux before and after a given event and is used as a quantitative descriptor of the degree of fouling that occurred. Figure 4 presents the flux recovery experienced by each membrane after 66 h of pressurized filtration of pretreated PW. The TFC Q_I membrane recovered much more of its flux than either NF90 trial and demonstrates that the TFC Q_I membrane fouled much less than the NF90 membrane during the filtration of pretreated PW. The minimal flux recovery observed in the NF90 membrane trials is similar to what has been observed elsewhere in the literature [37]. The similarity in flux recovery of the NF90 membrane during high- and low- pressure filtration suggests that hydrodynamic factors (i.e., permeate flux) were not the main cause of the observed fouling in the NF90 membrane trials. This is important to note given the significant difference in permeate flux between the NF90 and TFC Q_I membranes. To confirm that permeate flux did not play a

dominant role in the fouling of the NF90 membrane, fouling in the absence of permeate flux was studied via adsorption experiments.
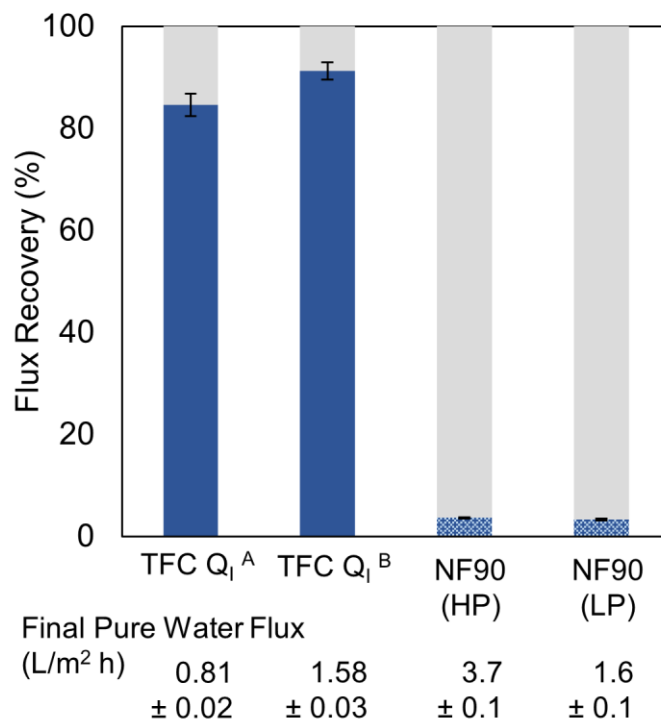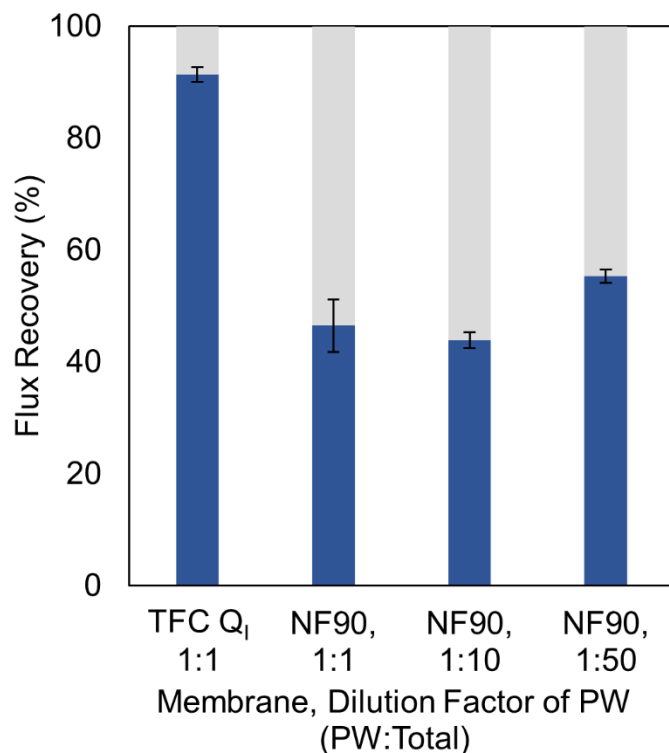

Figure 4. The flux recovery experienced by each membrane after 66 h of exposure to pretreated PW. The values shown represent the average of at least 3 replicate measurements in each experiment, with error bars representing 1 standard deviation. Below the graph are the pure water flux values after the 66-h exposure, with the error representing one standard deviation.

3.3 Fouling due to adsorption

Adsorption experiments enabled the study of membrane fouling in the absence of permeate flux [47,59]. While fouling associated with permeate flux is determined by the rates of solute transport to and from the membrane surface as influenced by the hydrodynamic conditions, fouling associated with adsorption is determined by the the physicochemical properties of the membrane (e.g., hydrophobicity, surface roughness) [47,57]. To study the fouling due to adsorption, a membrane was exposed to a given solution at the same cross-flow velocity as during filtration experiments, but at a transmembrane pressure (TMP) of 0 psi so that

there was no permeate flux through the membrane. This exposure lasted for 1 h. Flux recovery was used to describe the amount of fouling that occurred due to adsorption during this exposure. Membranes were exposed to two different solutions: First, membranes were exposed to a 15,000 mg/L aq. sodium chloride solution, a solution simulating the high TDS present in the pretreated PW. Second, membranes were exposed to the pretreated PW. None of the membranes experienced flux loss after exposure to the 15,000 mg/L aq. sodium chloride solution, suggesting that the fouling observed in the subsequent exposure to pretreated PW was due to the organic fraction rather than the salinity. Figure 5 shows the flux recovery after exposure to the pretreated PW. The TFC Q_I membrane's flux recovery after the 1 h exposure at 0 psi TMP (Figure 5) was similar to its flux recovery after the 66-h exposure at 400 psi TMP (Figure 4). This similarity suggests that adsorption of DOC can account for the majority of the fouling experienced by the TFC Q_I membrane during the filtration experiments. In the case of the NF90 membrane, the flux recovery after 1 h exposure at 0 psi TMP (Figure 5) was higher than after the 66-h exposure at 400 psi TMP (Figure 4), suggesting that DOC adsorption was one factor of multiple contributing to the fouling of the NF90 membrane during the filtration experiments. With a constant feed composition and the absence of permeate flux, the observed difference in flux recovery between the TFC Q_I membrane and the NF90 membrane must be due to the differences in the membrane materials themselves, in their physicochemical properties. Figure 5 shows that TFC Q_I membrane has a lower fouling propensity than the NF90 membrane.

Figure 5. The flux recovery experienced by the TFC Q_I and NF90 membranes exposed to various dilutions of pretreated PW for 1 h and 0 psi TMP. For the dilutions, the TDS was adjusted to 15,000 mg/L via the addition of sodium chloride. The values shown represent the average of at least 4 replicate measurements in each experiment, with error bars representing 1 standard deviation.

The DOC concentration present in this pretreated PW was much higher than the concentrations to which nanofiltration membranes are usually exposed and may explain the unexpectedly high degree of fouling observed in the NF90 membrane [37,39,58]. For this reason, the NF90 membrane was also exposed to pretreated PW in which the concentration of DOC was reduced via dilution. In these diluted samples, the original TDS concentration was maintained via the addition of sodium chloride so that only the DOC concentration varied. Figure 5 shows that no gain in flux recovery was achieved at a 1:10 dilution and that the flux recovery improved only slightly at a 1:50 dilution. The absence of improved flux recovery at these reduced DOC concentrations could be a result of the overall quantity of foulant in the feed volume relative to the membrane active area. The slight increase in flux recovery at a 1:50 dilution suggests that

further reduction of DOC concentrations would reduce fouling of the NF90 membrane.

Unfortunately, higher dilutions could not be investigated due to the detection limit of the TOC

machine combined with the machine's limits for TDS of the measured sample.

*3.4 Characterization of fouled membranes*

Water contact angle was used to evaluate the change in a membrane's surface due to

filtration of pretreated PW. Table 2 presents the contact angles of membranes exposed just to

water and aqueous sodium chloride solutions (membrane controls) and the contact angle of

membranes exposed to 66 h of pressurize filtration of pretreated PW. Any difference in water

contact angle between the control and exposed sample was attributed to fouling of the membrane

by the pretreated PW. As can be seen in Table 2, the contact angles of the exposed TFC Q_I

membranes were within one standard deviation of that of the control. The absence of a

significant change in membrane hydrophobicity is not surprising given that the TFC Q_I

membrane recovered most of its flux and had minimal fouling. Similarly, the contact angle of the

NF90 (LP) was similar to the NF90 control. There are two possible conclusions from these

results: 1.) there is insufficient amount of foulant on the membrane surface to change the surface

hydrophobicity, or 2.) the hydrophobicity of the foulant is the same as that of the membrane

surface. The surface of NF90 (HP), however, does become more hydrophobic due to exposure to

pretreated PW, demonstrating that the foulant in the case of NF90 (HP) is hydrophobic in nature.

Table 2. The water contact angle of dry membranes, as measured by the sessile drop method. Values are averages of two measurements, with the error representing one standard deviation.

Membrane ID	Contact Angle (degrees)
TFC Q_I control	63 ± 1
TFC Q_I [A]	61 ± 4
TFC Q_I [B]	70 ± 10

NF90 control	76 ± 6
NF90 (HP)	91 ± 4
NF90 (LP)	77 ± 2

Chemical analysis was used to study the nature of the foulants left on the membrane surface after the 66-h pressurized filtration. Elemental analysis of the fouled membrane selective layer surface by EDS showed the absence of inorganic compounds, supporting the conclusion that the fouling agents were organic in nature. Because the membrane materials themselves were also organic in nature, EDS could not distinguish between the organic foulant and the organic membrane to confirm the presence of the organic foulant. Therefore, confirmation of the presence of an organic fouling layer was pursued via ATR-FTIR spectroscopy [36,37,58], which can differentiate organic materials by functional group. Figure 6 presents the FTIR spectra of the pristine and fouled membranes. The increased intensity of the peaks just below 3000 cm^{-1} in the fouled NF90 membrane samples as compared to the pristine NF90 membrane sample suggests the presence of fouling [42]. The absence of other peaks associated with the foulant is not surprising because the NF90 membrane itself had such a strong signal. Prior publications have also noted the absence of variation in FTIR spectra of the NF90 membrane despite an observed decrease in flux associated with fouling [37,58]. The TFC Q_I membrane had strong FTIR peaks around 3000 cm^{-1}, preventing the detection of any small changes due to organic fouling in this spectral region.
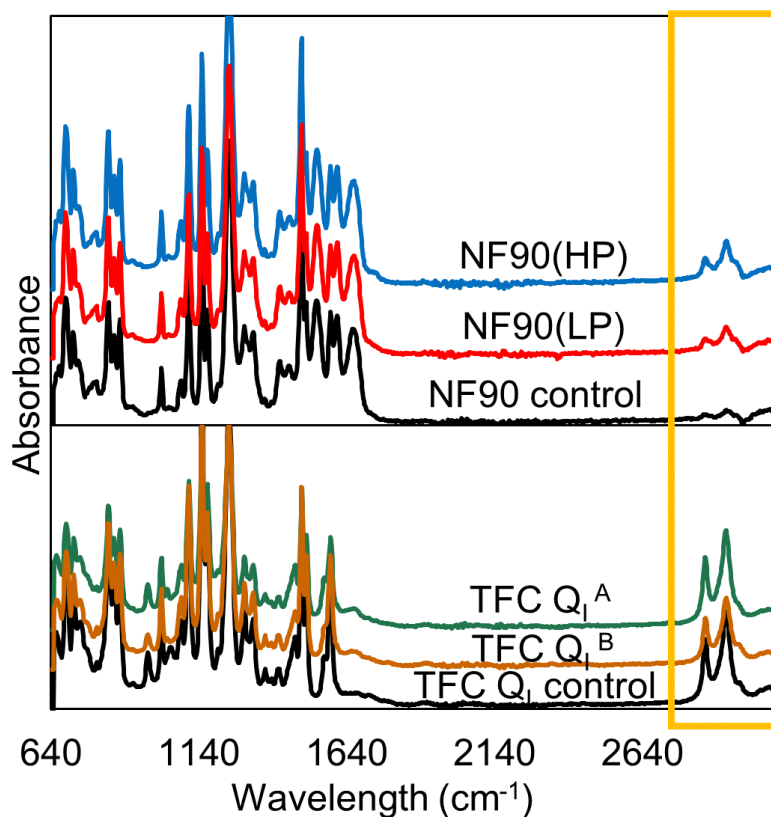
Figure 6. ATR-FTIR spectra of the NF90 and TFC Q_I membranes, both pristine (i.e., control samples) and fouled after 66 h of pressurized filtration of pretreated PW.

A comparison of the flux recoveries in Figure 4 shows that the TFC Q_I membrane fouled less than the NF90 membrane during cross-flow filtration of this pretreated PW. A comparison of the flux recoveries in Figure 5 shows that this difference in fouling was due in large part to differences in DOC adsorption. The conclusion that the foulant was organic in nature is further substantiated by the analysis of the membrane surfaces discussed above. DOC adsorbs to the membrane as a result of its affinity for membrane, which is determined by the physicochemical properties of the membrane. Cumulatively, these results suggest that the physicochemical properties of the NF90 membrane caused the membrane to foul in the presence of this pretreated PW while the physicochemical properties of the TFC Q_I membrane mitigated fouling to a large

degree. While it is unexpected for nanofiltration membranes to maintain their performance in the presence of such high concentrations of DOC, the TFC Q_I membrane did maintain most of its performance in such conditions, making feasible a treatment train in which desalination occurs before removal of the DOC.

3.4 Discussion of fouling propensity

Differences in fouling propensity between membranes arise from differences in their physicochemical properties. Research has shown that surface roughness promotes membrane fouling [11,12,42,60]. Herein, SEM was used to compare the surface morphology of the NF90 membrane to that of the TFC Q_I membrane (Figure 7). The smoother surface of the TFC Q_I membrane suggests that the TFC Q_I membrane would have a lower fouling propensity than the NF90 membrane. Electrostatic repulsion has also been shown to be an important variable for minimizing fouling [11,61]. The TFC Q_I membrane has a much higher charge density (calculated to be about 1,640 mol/m^3, see Section 3 in the Data in Brief) than the NF90 membrane (estimated around 1 mol/m^3 [62]) and thereby should induce greater electrostatic repulsion, further contributing to its lower fouling propensity. Lastly, research has shown that periodic nanostructure reduces fouling [15]. The periodic nanostructure of the TFC Q_I membrane likely contributed to its reduced fouling propensity relative to the amorphous NF90 membrane. In summary, the surface smoothness, high charge density, and periodic nanostructure of the TFC Q_I membrane likely all contribute to the explanation of its reduced fouling propensity relative to the NF90 membrane.
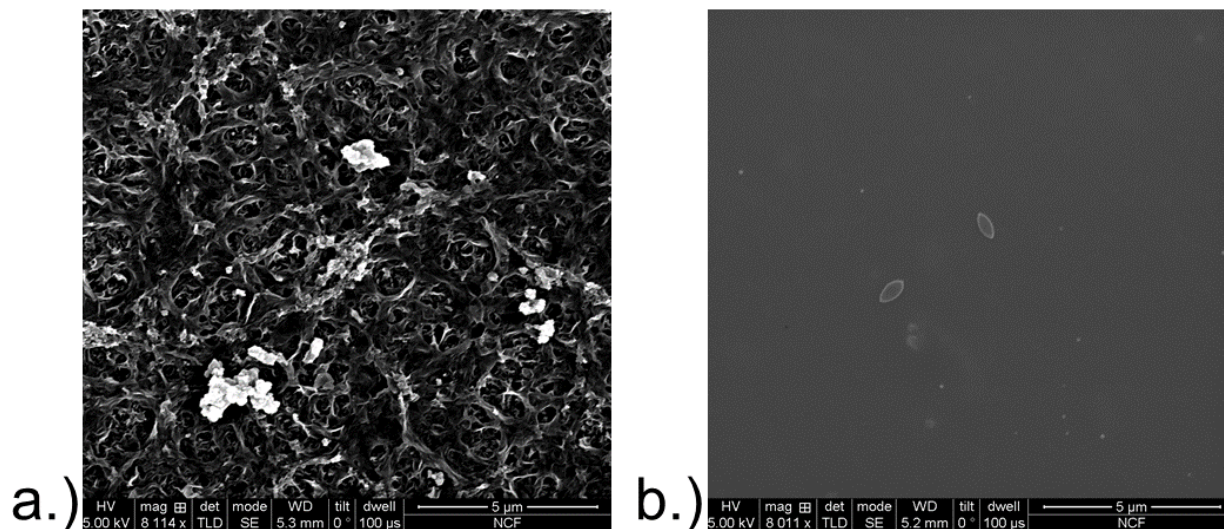
Figure 7. SEM images of: a.) a pristine NF90 membrane, and b.) a pristine TFC Q_I membrane.

The NF90 membrane was chosen as a commercial comparison for this study because it has been previously used for hydraulic fracturing wastewater treatment studies and because it has a selectivity in the range of interest [37,39]. While industry widely uses the NF90 membrane, this membrane is by no means the standard for fouling. The NF90 membrane has a rougher surface and is more hydrophobic than other commercial NF and RO membranes [58,63,64], and therefore often exhibits worse fouling than many membranes [37,58,64]. Therefore, future investigations should include comparisons to a range of commercial polymeric membranes in order to elucidate the difference in fouling propensity and selectivity between the TFC Q_I membrane and current commercial polyamide-based membranes.

4. Conclusions

The TFC Q_I membrane is a recently-developed nanoporous polymer membrane with a well-defined periodic nanopore structure that enables a unique selectivity for low-molecular-weight organic solutes over salts. Herein, the TFC Q_I membrane filtered pretreated PW for 66 h using cross-flow filtration. The results of this work, both in terms of thickness-normalized water flux and selectivity, demonstrate that the TFC Q_I membrane maintained its performance in industrially-relevant conditions. In terms of selectivity, thickness-normalized water flux, and flux recovery, the TFC Q_I membrane out-performed the commercial NF90 membrane. Since flux recovery is a descriptor of fouling experienced by the membrane, these results demonstrate that the TFC Q_I membrane fouled less than the NF90 membrane under the set of conditions used herein. Considering the difference in flux recovery after adsorption experiments, the lower fouling propensity of the TFC Q_I membrane as compared to the NF90 membrane is attributed to its physicochemical properties. This performance by the TFC Q_I membrane exhibits its competitiveness with a current commercial membrane. The TFC Q_I membrane's reduced fouling propensity in conjunction with its selectivity makes feasible a treatment approach in which desalination occurs before biodegradation. While the TFC Q_I membrane is not yet ready for commercialization, this work motivates the further development of this material for industrial applications. This work also warrants further study of the physicochemical properties of the TFC Q_I membrane that give rise to its unique performance.

Acknowledgments

References

[1]   M. Elimelech, W.A. Phillip, The future of seawater and the environment: Energy, technology, and the environment, Science 333 (2011) 712–718. doi:10.1126/science.1200488.

[2]   G.M. Geise, D.R. Paul, B.D. Freeman, Fundamental water and salt transport properties of polymeric materials, Prog. Polym. Sci. 39 (2014) 1–24. doi:10.1016/j.progpolymsci.2013.07.001.

[3]   D.J. Miller, X. Huang, H. Li, S. Kasemset, A. Lee, D. Agnihotri, T. Hayes, D.R. Paul, B.D. Freeman, Fouling-resistant membranes for the treatment of flowback water from hydraulic shale fracturing: A pilot study, J. Membr. Sci. 437 (2013) 265–275. doi:10.1016/j.memsci.2013.03.019.

[4]   J.R. Werber, C.O. Osuji, M. Elimelech, Materials for next-generation desalination and water purification membranes, Nat. Rev. Mater. (2016) 16018. doi:10.1038/natrevmats.2016.18.

[5]   H.B. Park, J. Kamcev, L.M. Robeson, M. Elimelech, B.D. Freeman, Maximizing the right stuff: The trade-off between membrane permeability and selectivity, Science 356 (2017). doi:10.1126/science.aab0530.

[6]   G.M. Geise, H.-S. Lee, D.J. Miller, B.D. Freeman, J.E. McGrath, D.R. Paul, Water purification by membranes: The role of polymer science, J. Polym. Sci. Part B Polym. Phys. 48 (2010) 1685–1718. doi:10.1002/polb.

[7]   A.W. Mohammad, Y.H. Teow, W.L. Ang, Y.T. Chung, D.L. Oatley-Radcliffe, N. Hilal, Nanofiltration membranes review: Recent advances and future prospects, Desalination 356 (2015) 226–254. doi:10.1016/j.desal.2014.10.043.

[8]   B. Van der Bruggen, M. Mänttäri, M. Nyström, Drawbacks of applying nanofiltration and how to avoid them: A review, Sep. Purif. Technol. 63 (2008) 251–263. doi:10.1016/j.seppur.2008.05.010.

[9]   M. Ulbricht, Advanced functional polymer membranes, Polymer 47 (2006) 2217–2262. doi:10.1016/j.polymer.2006.01.084.

[10]   C.Y. Tang, T.H. Chong, A.G. Fane, Colloidal interactions and fouling of NF and RO membranes: A review, Adv. Colloid Interface Sci. 164 (2011) 126–143. doi:10.1016/j.cis.2010.10.007.

[11]   S. Hong, M. Elimelech, Chemical and physical aspects of natural organic matter (NOM) fouling of nanofiltration membranes, J. Membr. Sci. 132 (1997) 159–181. doi:10.1016/S0376-7388(97)00060-4.

[12]   E.M. Vrijenhoek, S. Hong, M. Elimelech, Influence of membrane surface properties on initial rate of colloidal fouling of reverse osmosis and nanofiltration membranes, J. Membr. Sci. 188 (2001)

115–128. doi:10.1016/S0376-7388(01)00376-3.

[13]   B.M. Carter, B.R. Wiesenauer, E.S. Hatakeyama, J.L. Barton, R.D. Noble, D.L. Gin, Glycerol-based bicontinuous cubic lyotropic liquid crystal monomer system for the fabrication of thin-film membranes with uniform nanopores, Chem. Mater. 24 (2012) 4005–4007. doi:10.1021/cm302027s.

[14]   S.M. Dischinger, J. Rosenblum, R.D. Noble, D.L. Gin, K.G. Linden, Application of a lyotropic liquid crystal nanofiltration membrane for hydraulic fracturing flowback water: selectivity and implications for treatment, J. Membr. Sci. 543 (2017) 319–327. doi:10.1016/j.memsci.2017.08.028.

[15]   E.S. Hatakeyama, H. Ju, C.J. Gabriel, J.L. Lohr, J.E. Bara, R.D. Noble, B.D. Freeman, D.L. Gin, New protein-resistant coatings for water filtration membranes based on quaternary ammonium and phosphonium polymers, J. Membr. Sci. 330 (2009) 104–116. doi:10.1016/j.memsci.2008.12.049.

[16]   G. Kang, Y. Cao, H. Zhao, Q. Yuan, Preparation and characterization of crosslinked poly (ethylene glycol) diacrylate membranes with excellent antifouling and solvent-resistant properties, J. Membr. Sci. 318 (2008) 227–232. doi:10.1016/j.memsci.2008.02.045.

[17]   Y. Lester, I. Ferrer, E.M. Thurman, K.A. Sitterley, J.A. Korak, G. Aiken, K.G. Linden, Characterization of hydraulic fracturing flowback water in Colorado: Implications for water treatment, Sci. Total Environ. 512–513 (2015) 637–644. doi:10.1016/j.scitotenv.2015.01.043.

[18]   J. Rosenblum, A.W. Nelson, B. Ruyle, M.K. Schultz, J.N. Ryan, K.G. Linden, Temporal characterization of flowback and produced water quality from a hydraulically fractured oil and gas well, Sci. Total Environ. 596–597 (2017) 369–377. doi:10.1016/j.scitotenv.2017.03.294.

[19]   A.J. Kondash, N.E. Lauer, A. Vengosh, The intensification of the water footprint of hydraulic fracturing, Sci. Adv. 4 (2018). doi:10.1126/sciadv.aar5982.

[20]   A. Fakhru'l-Razi, A. Pendashteh, L.C. Abdullah, D.R.A. Biak, S.S. Madaeni, Z.Z. Abidin, Review of technologies for oil and gas produced water treatment, J. Hazard. Mater. 170 (2009) 530–551. doi:10.1016/j.jhazmat.2009.05.044.

[21]   D.L. Shaffer, L.H. Arias Chavez, M. Ben-Sasson, S.R.V. Castrillon, N.Y. Yip, M. Elimelech, Desalination and reuse of high-salinity shale gas produced water : Drivers, technologies, and future directions, Environ. Sci. Technol. 47 (2013) 9569–9583.

[22]   K.B. Gregory, R.D. Vidic, D.A. Dzombak, Water management challenges associated with the production of shale gas by hydraulic fracturing, Elements 7 (2011) 181–186. doi:10.2113/gselements.7.3.181.

[23]   C.D. Kassotis, L.R. Iwanowicz, D.M. Akob, I.M. Cozzarelli, A.C. Mumford, W.H. Orem, S.C. Nagel, Endocrine disrupting activities of surface water associated with a West Virginia oil and gas industry wastewater disposal site, Sci. Total Environ. 557–558 (2016) 901–910. doi:10.1016/j.scitotenv.2016.03.113.

[24]   M. Weingarten, S. Ge, J.W. Godt, B.A. Bekins, J.L. Rubinstein, High-rate injection is associated with the increase in U.S. mid-continent seismicity, Science 348 (2015) 1336–1340. doi:10.1126/science.aab1345.

[25]   S. Alzahrani, A.W. Mohammad, Challenges and trends in membrane technology implementation for produced water treatment: A review, J. Water Process Eng. 4 (2014) 107–133. doi:10.1016/j.jwpe.2014.09.007.

[26]   S.M. Riley, D.C. Ahoor, K. Oetjen, T.Y. Cath, Closed circuit desalination of O&G produced water: An evaluation of NF/RO performance and integrity, Desalination 442 (2018) 51–61. doi:10.1016/j.desal.2018.05.004.

[27]   R.W. Baker, Membrane Technology and Applications, Third Edit, John Wiley & Sons, Ltd, 2012.

[28]   P. Xu, J.E. Drewes, Viability of nanofiltration and ultra-low pressure reverse osmosis membranes for multi-beneficial use of methane produced water, Sep. Purif. Technol. 52 (2006) 67–76. doi:10.1016/j.seppur.2006.03.019.

[29]   P. Westerhoff, S. Lee, Y. Yang, G.W. Gordon, K. Hristovski, R.U. Halden, P. Herckes, Characterization, recovery opportunities, and valuation of metals in municipal sludges from U.S.

wastewater treatment plants nationwide, Environ. Sci. Technol. 49 (2015) 9479–9488. doi:10.1021/es505329q.

[30]   S. Zhang, P. Wang, X. Fu, T.S. Chung, Sustainable water recovery from oily wastewater via forward osmosis-membrane distillation (FO-MD), Water Res. 52 (2014) 112–121. doi:10.1016/j.watres.2013.12.044.

[31]   A. Butkovskyi, A.H. Faber, Y. Wang, K. Grolle, R. Hofman-Caris, H. Bruning, A.P. Van Wezel, H.H.M. Rijnaarts, Removal of organic compounds from shale gas flowback water, Water Res. 138 (2018) 47–55. doi:10.1016/j.watres.2018.03.041.

[32]   S.M. Riley, D.C. Ahoor, J. Regnery, T.Y. Cath, Tracking oil and gas wastewater-derived organic matter in a hybrid biofilter membrane treatment system: A multi-analytical approach, Sci. Total Environ. 613–614 (2018) 208–217. doi:10.1016/j.scitotenv.2017.09.031.

[33]   Y. Lester, T. Yacob, I. Morrissey, K.G. Linden, Can we treat hydraulic fracturing flowback with a conventional biological process? The case of guar gum, Environ. Sci. Technol. Lett. 1 (2013) 133–136. doi:10.1021/ez4000115.

[34]   E. Reid, X. Liu, S.J. Judd, Effect of high salinity on activated sludge characteristics and membrane permeability in an immersed membrane bioreactor, J. Membr. Sci. 283 (2006) 164–171. doi:10.1016/j.memsci.2006.06.021.

[35]   O. Lefebvre, R. Moletta, Treatment of organic pollution in industrial saline wastewater: A literature review, Water Res. 40 (2006) 3671–3682. doi:10.1016/j.watres.2006.08.027.

[36]   S. Alzahrani, A.W. Mohammad, N. Hilal, P. Abdullah, O. Jaafar, Identification of foulants, fouling mechanisms and cleaning efficiency for NF and RO treatment of produced water, Sep. Purif. Technol. 118 (2013) 324–341. doi:10.1016/j.seppur.2013.07.016.

[37]   S. Mondal, S.R. Wickramasinghe, Produced water treatment by nanofiltration and reverse osmosis membranes, J. Membr. Sci. 322 (2008) 162–170. doi:10.1016/j.memsci.2008.05.039.

[38]   E.S. Kim, Y. Liu, M.G. El-Din, The effects of pretreatment on nanofiltration and reverse osmosis membrane filtration for desalination of oil sands process-affected water, Sep. Purif. Technol. 81 (2011) 418–428. doi:10.1016/j.seppur.2011.08.016.

[39]   S.M. Riley, J.M.S. Oliveira, J. Regnery, T.Y. Cath, Hybrid membrane bio-systems for sustainable treatment of oil and gas produced water and fracturing flowback water, Sep. Purif. Technol. 171 (2016) 297–311. doi:10.1016/j.seppur.2016.07.008.

[40]   C. Guo, H. Chang, B. Liu, Q. He, B. Xiong, M. Kumar, A.L. Zydney, A combined ultrafiltration-reverse osmosis process for external reuse of Weiyuan shale gas flowback and produced water, Environ. Sci. Water Res. Technol. 4 (2018) 942–955. doi:10.1039/c8ew00036k.

[41]   R.A. Maltos, J. Regnery, N. Almaraz, S. Fox, M. Schutter, T.J. Cath, M. Veres, B.D. Coday, T.Y. Cath, Produced water impact on membrane integrity during extended pilot testing of forward osmosis – reverse osmosis treatment, Desalination 440 (2018) 99–110. doi:10.1016/j.desal.2018.02.029.

[42]   E.A. Bell, T.E. Poynor, K.B. Newhart, J. Regnery, B.D. Coday, T.Y. Cath, Produced water treatment using forward osmosis membranes: Evaluation of extended-time performance and fouling, J. Membr. Sci. 525 (2017) 77–88. doi:10.1016/j.memsci.2016.10.032.

[43]   T. Sakamoto, T. Ogawa, H. Nada, K. Nakatsuji, M. Mitani, B. Soberats, K. Kawata, M. Yoshio, H. Tomioka, T. Sasaki, M. Kimura, M. Henmi, T. Kato, Development of nanostructured water treatment membranes based on thermotropic liquid crystals: molecular design of sub-nanoporous materials, Adv. Sci. 1700405 (2017) 1–9. doi:10.1002/advs.201700405.

[44]   M. Henmi, K. Nakatsuji, T. Ichikawa, H. Tomioka, T. Sakamoto, M. Yoshio, T. Kato, Self-organized liquid-crystalline nanostructured membranes for water treatment: Selective permeation of ions, Adv. Mater. 24 (2012) 2238–2241. doi:10.1002/adma.201200108.

[45]   S.M. Dischinger, M.J. McGrath, K.R. Bourland, R.D. Noble, D.L. Gin, Effect of post-polymerization anion-exchange on the rejection of uncharged aqueous solutes in nanoporous, ionic, lyotropic liquid crystal polymer membranes, J. Membr. Sci. 529 (2017) 72–79. doi:10.1016/j.memsci.2017.01.049.

[46]   B.M. Carter, B.R. Wiesenauer, R.D. Noble, D.L. Gin, Thin-film composite bicontinuous cubic lyotropic liquid crystal polymer membranes: Effects of anion-exchange on water filtration performance, J. Membr. Sci. 455 (2014) 143–151. doi:10.1016/j.memsci.2013.12.056.

[47]   D.J. Miller, S. Kasemset, D.R. Paul, B.D. Freeman, Comparison of membrane fouling at constant flux and constant transmembrane pressure conditions, J. Membr. Sci. 454 (2014) 505–515. doi:10.1016/j.memsci.2013.12.027.

[48]   E. Negaresh, A. Antony, M. Bassandeh, D.E. Richardson, G. Leslie, Selective separation of contaminants from paper mill effluent using nanofiltration, Chem. Eng. Res. Des. 90 (2012) 576–583. doi:10.1016/j.cherd.2011.08.005.

[49]   L. Lin, R. Lopez, G.Z. Ramon, O. Coronell, Investigating the void structure of the polyamide active layers of thin-film composite membranes, J. Membr. Sci. 497 (2016) 365–376. doi:10.1016/j.memsci.2015.09.020.

[50]   T.C. Huang, H. Toraya, T.N. Blanton, Y. Wu, X-ray powder diffraction analysis of silver behenate, a possible low-angle diffraction standard, J. Appl. Crystallogr. 26 (1993) 180–184. doi:10.1107/S0021889892009762.

[51]   American Public Health Association, Standard Methods for the Examination of Water and Wastewater, American Public Health Association, 2005.

[52]   J.S. Rosenblum, K.A. Sitterley, E.M. Thurman, I. Ferrer, K.G. Linden, Hydraulic fracturing wastewater treatment by coagulation-adsorption for removal of organic compounds and turbidity, J. Environ. Chem. Eng. 4 (2016) 1978–1984. doi:10.1016/j.jece.2016.03.013.

[53]   J. Rosenblum, E.M. Thurman, I. Ferrer, G. Aiken, K.G. Linden, Organic chemical characterization and mass balance of a hydraulically fractured well: From fracturing fluid to produced water over 405 days, Environ. Sci. Technol. 51 (2017) 14006–14015. doi:10.1021/acs.est.7b03362.

[54]   E. Barbot, N.S. Vidic, K.B. Gregory, R.D. Vidic, Spatial and temporal correlation of water quality parameters of produced waters from devonian-age shale follwoing hydraulic fracturing, Environ. Sci. Technol. 47 (2013) 2562–2569. http://dx.doi.org/10.1021/es304638h.

[55]   C.H. Koo, A.W. Mohammad, F. Suja', M.Z. Meor Talib, Review of the effect of selected physicochemical factors on membrane fouling propensity based on fouling indices, Desalination 287 (2012) 167–177. doi:10.1016/j.desal.2011.11.003.

[56]   C. Thamaraiselvan, N. Michael, Y. Oren, Selective separation of dyes and brine recovery from textile wastewater by nanofiltration membranes, Chem. Eng. Technol. 41 (2018) 185–293. doi:10.1002/ceat.201700373.

[57]   B. Van Der Bruggen, C. Vandecasteele, Flux decline during nanofiltration of organic components in aqueous solution, Environ. Sci. Technol. 35 (2001) 3535–3540. doi:10.1021/es0100064.

[58]   P. Xu, C. Bellona, J.E. Drewes, Fouling of nanofiltration and reverse osmosis membranes during municipal wastewater reclamation: Membrane autopsy results from pilot-scale investigations, J. Membr. Sci. 353 (2010) 111–121. doi:10.1016/j.memsci.2010.02.037.

[59]   R.W. Field, G.K. Pearce, Critical, sustainable and threshold fluxes for membrane filtration with water industry applications, Adv. Colloid Interface Sci. 164 (2011) 38–44. doi:10.1016/j.cis.2010.12.008.

[60]   G. Mustafa, K. Wyns, A. Buekenhoudt, V. Meynen, New insights into the fouling mechanism of dissolved organic matter applying nanofiltration membranes with a variety of surface chemistries, Water Res. 93 (2016) 195–204. doi:10.1016/j.watres.2016.02.030.

[61]   A.S. Al-Amoudi, Factors affecting natural organic matter (NOM) and scaling fouling in NF membranes: A review, Desalination 259 (2010) 1–10. doi:10.1016/j.desal.2010.04.003.

[62]   K. Zhao, Q. Lu, W. Su, Estimation of electrical parameters inside nanofiltration membranes in various electrolyte solutions by dielectric spectroscopy analysis, RSC Adv. 4 (2014) 63085–63099. doi:10.1039/c4ra13598a.

[63]   N. Hilal, H. Al-Zoubi, N.A. Darwish, A.W. Mohammad, Characterisation of nanofiltration membranes using atomic force microscopy, Desalination 177 (2005) 187–199. doi:10.1016/j.desal.2004.12.008.

[64] K. Boussu, Y. Zhang, J. Cocquyt, P. Van der Meeren, A. Volodin, C. Van Haesendonck, J.A. Martens, B. Van der Bruggen, Characterization of polymeric nanofiltration membranes for systematic analysis of membrane performance, J. Membr. Sci. 278 (2006) 418–427. doi:10.1016/j.memsci.2005.11.027.